Eur. Phys. J. A **31**, 522–526 (2007)
DOI 10.1140/epja/i2006-10230-6

THE EUROPEAN
PHYSICAL JOURNAL A

Special Article – QNP 2006

Measurement of pionium lifetime with the Dirac spectrometer

B. Adeva[a], A. Romero Vidal, and O. Vázquez Doce

IGFAE, Universidade de Santiago de Compostela, 15706 Santiago de Compostela, Spain

Received: 8 November 2006
Published online: 5 March 2007 –

Abstract. Pionium ($\pi^+\pi^-$ bound state) lifetime is measured with improved precision with respect to earlier work, and the $\pi\pi$ s-wave scattering length difference between $I = 0$ and $I = 2$ amplitudes $|a_0 - a_2|$ is determined to 5% precision.

PACS. 13.75.Lb Meson-meson interactions – 12.39.Fe Chiral Lagrangians

1 Introduction

Pionium is a Coulomb $\pi^+\pi^-$ bound state, with Bohr radius $r_B = 387\,\mathrm{fm}$. Its ground state ($1s$) lifetime τ_{1s} is dominated by the short-range reaction $\pi^+\pi^- \to \pi^0\pi^0$, which largely exceeds the $\gamma\gamma$ decay, neglected in the present analysis:

$$\Gamma = \frac{1}{\tau} = \Gamma_{2\pi^0} + \Gamma_{\gamma\gamma} \qquad (1)$$

with $\frac{\Gamma_{\gamma\gamma}}{\Gamma_{2\pi^0}} \sim 4 \times 10^{-3}$. At lowest order in QCD and QED, the total width can be expressed as a function of the s-wave $I = 0$ (a_0) and $I = 2$ (a_2) $\pi\pi$ scattering lengths and the next-to-leading order has been calculated

$$\Gamma_{1s} = \frac{1}{\tau_{1s}} = \frac{2}{9}\alpha^3 p |a_0 - a_2|^2 (1 + \delta)\ M^2_{\pi^+}\,, \qquad (2)$$

where $p = \sqrt{M^2_{\pi^+} - M^2_{\pi^0} - \frac{1}{4}\alpha^2 M^2_{\pi}}$. A significant correction $\delta = (5.8 \pm 1.2) \times 10^{-2}$ arises with respect to lowest order, once a non-singular relativistic amplitude at threshold is built [1]. Therefore a 5% precision can be achieved in the measurement of $|a_0 - a_2|$ provided a 10% lifetime error is reached. Note should be taken that this method implies access to the physical reaction threshold (Bohr momentum $P_B \sim 0.5\,\mathrm{MeV}/c$). The $\pi\pi$ scattering lengths have been calculated in the framework of chiral perturbation theory with small errors [2]. Independently, a self-consistent representation of these amplitudes has been recently evaluated [3]. The former implies a lifetime prediction $\tau_{1s} = 2.9 \pm 0.1\,\mathrm{fs}$. There exists an ample and detailed literature about the chiral expansion of $\pi\pi$ amplitudes, including error estimates from experimental parameter uncertainies [4].

Pionium, with 4-momentum $p_A = (E_A, \boldsymbol{p}_A)$, is produced by Coulomb final-state interaction in ns states according to the expression

$$\frac{\mathrm{d}\sigma}{\mathrm{d}\boldsymbol{p}_A} = (2\pi)^3 \frac{E_A}{2M_\pi} |\psi_n(0)|^2 \left(\frac{\mathrm{d}\sigma^0_s}{\mathrm{d}\boldsymbol{p}_1 \mathrm{d}\boldsymbol{p}_2}\right)_{\boldsymbol{p}_1=\boldsymbol{p}_2=\boldsymbol{p}_A/2}, \qquad (3)$$

where σ^0_s denotes the Coulomb-uncorrected semi-inclusive $\pi^+\pi^-$ cross-section [5], which is enhanced by a high-energy and high-intensity proton beam colliding on a nuclear target foil.

Produced atoms propagate inside the target foil (decay length is only a few microns) before they are ionized (broken up) into $\pi^+\pi^-$ pairs in the continuum spectrum, which are subsequently triggered and detected by the DIRAC spectrometer. Due to the very small momentum transfer induced by the electric field near the target nuclei, the signal is detected as an excess with respect to the $\pi^+\pi^-$ Coulomb-correlated spectrum at very low center-of-mass momentum $Q(\sim 0.5\,\mathrm{MeV}/c)$.

A first measurement of pionium lifetime was published by DIRAC with extremely conservative error assesment [6]. Considerable work has taken place since then, and the results presented here arise from a better knowledge of the main error sources, as well as from a complete use of the spectrometer detectors.

2 Spectrometer setup

DIRAC is a double-arm spectrometer [7] where $\pi^+\pi^-$ pairs are collected into a narrow window of $10 \times 10\,\mathrm{cm}^2$ aperture at $2.5\,\mathrm{m}$ from the target foil, and then split by a $1.65\,\mathrm{T}$ dipole magnet. It is installed at the East Hall $24\,\mathrm{GeV}/c$ proton beam line of CERN PS. A top view is depicted in fig. 1. The spectrometer acceptance is elevated by $5.7°$ with respect to the beam line, in order to avoid backgrounds from the induced radiation. The beam was normally operated at 10^{11} protons per spill.

[a] e-mail: adevab@usc.es

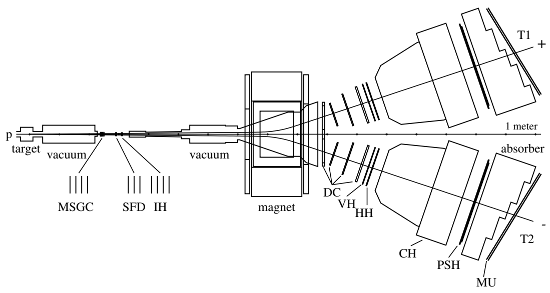

Fig. 1. Top view of the DIRAC spectrometer.

In addition to the double arm downstream the magnet, an upstream arm has been built with the following purpose:

- Improve the Q_T and Q_L resolution by measuring the two-pion opening angle, thus reducing background and pion decay path.
- Perform identification of very close pairs by means of pulse-height analysis of double ionization.

The upstream arm is composed by 4 MSGC/GEM planes, 2 Scintillator Fibre Detectors (SFD) and 4 Ionization Hodoscope (IH) planes. A third SFD was introduced in 2002 and 2003 runs.

The downstream two-arm spectrometer is made of 5 fast Drift Chambers (DC) as main tracking detector, two Cherenkov counters (CH) to provide efficient electron veto, a high-resolution Vertical Hodoscope (VH) system as Time-of-Flight (TOF) detector, Horizontal Hodoscopes (HH) to trigger horizontal splitting, Pre-Shower detectors (PSH) for further electron rejection and Muon Counters (MU) to veto pion decays.

The whole setup provides Q_T and Q_L resolutions of $0.1\,\text{MeV}/c$ and $0.5\,\text{MeV}/c$ respectively. Due to the small pionium rate compared to the Coulomb interacting background, low-Q selection ($Q < 30\,\text{MeV}/c$) must be achieved at trigger level with uniform acceptance, which requires a sophisticated multi-level structure. Wide TOF trigger cuts are applied, in order to accept a sizeable fraction of accidental pairs. In addition, asymmetric triggers are used to select $\Lambda \to p\pi^-$ decay for calibration purposes (Λ mass resolution is $\sigma_\Lambda = 0.395\,\text{MeV}/c^2$).

3 Reconstruction method

Pions are reconstructed in DIRAC after performing independent tracking in the upstream and downstream arms. The opening angle is determined with high precision (only limited by multiple scattering inside the target) making use of 4 MSGC/GEM detectors, in conjuntion with TDC information from SFD.

Upstream track pairs are matched in space and time with DC tracks with uniform matching efficiency. When only a single unresolved track can be matched, a double-ionization pulse-height signal is required in IH.

A high-precision TOF measurement ($\sim 170\,\text{ps}$) is provided by the VH, which allows to perform clean separation between time-correlated (prompt) pairs and accidental pairs coming from different proton-nucleus interactions (see fig. 2). Under the prompt peak in the Δt spectrum we find both the real Coulomb-correlated pairs and the corresponding pionium signal fraction. It is, however, inevitable (despite the excellent time resolution) that a fraction of non-Coulomb pairs are also selected, arising from inclusive pion "long lifetime" decays in the subpicosecond range. Of course, the accidental pair fraction can be determined in addition from fig. 2.

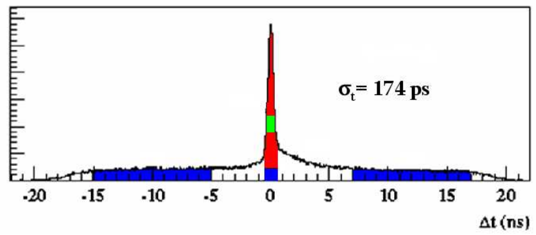

Fig. 2. Time difference between the negative and positive arms measured by the vertical hodoscope. The central peak corresponds to prompt events and the dark region to accidental pairs.

Prompt experimental pairs are finally selected for the analysis with relative momentum cuts $|Q_L| < 20\,\text{MeV}/c$ and $Q_T < 5\,\text{MeV}/c$. Protons are removed with a $P_+ > 4\,\text{GeV}/c$ cut over the positive arm.

4 Analysis of Q-spectrum

The prompt two-pion spectrum in (Q_T, Q_L)-plane has been χ^2-analysed by comparison with the following input spectra:

- Monte Carlo describing the *Coulomb* final-state interaction (CC) by means of the Sakharov-Gamow factor $A_C(Q) = 2\pi(p_B/Q)/(1 - \exp(-2\pi p_B/Q))$, p_B being the pion Bohr momentum.
- Monte Carlo describing *accidental* coincidences taken by the spectrometer (AC), simulated isotropically in their center-of-mass frame.
- Monte Carlo describing *non-Coulomb* $\pi^+\pi^-$ pairs (NC). It simulates the additional fraction of events from decay of long-lifetime resonances which are still detected as time correlated. In practice, it differs from the previous one very slightly, only for the different lab frame pion momentum spectrum.
- Pionium *atom* Monte Carlo model (AA) which is used to cross-check and fit the observed deviation with respect to the continuum background constructed from the previous Monte Carlo input.

The laboratory frame pair momentum spectrum has been generated according to the one really observed with spectrometer data.

A two-dimensional analysis of the $\pi^+\pi^-$ spectrum in the center-of-mass frame has been carried out, choosing the transverse $Q_T = \sqrt{Q_X^2 + Q_Y^2}$ and longitudinal $Q_L =$

$|Q_Z|$ components (with respect to the pair direction of flight Z) as independent variables. The analysis has been done independently at ten individual 600 MeV/c bins of the lab frame momentum p of the pair.

The total number of events used for the above Monte Carlo samples are denoted by N_{CC}, N_{AC}, N_{NC} and N_{AA} respectively, whereas N_p represents the total number of prompt events in the analysis, under the reference cuts $Q_T < 5\,\mathrm{MeV}/c$ and $Q_L < 20\,\mathrm{MeV}/c$. Index k runs over all (i,j) bins of the (Q_T, Q_L) histograms, and we denote by N^k_{CC} the number of Coulomb events observed in each particular bin (i,j). Similarly for the other input spectra, namely N^k_{AC}, N^k_{NC} and N^k_{AA}. Normalised spectra are used to fit the data, and we denote them by small letters, $n^k_{CC} = N^k_{CC}/N_{CC}$ and likewise for the rest. The ratios $x_{CC} = N_{CC}/N_p$, $x_{AC} = N_{AC}/N_p$, $x_{NC} = N_{NC}/N_p$ and $x_{AA} = N_{AA}/N_p$ help define the statistical errors. The χ^2 analysis is based upon the expression

$$\chi^2 = \sum_k \frac{\left(N^k_p - \beta\alpha_1 n^k_{CC} - \beta\alpha_2 n^k_{AC} - \beta\alpha_3 n^k_{NC} - \beta\gamma n^k_{AA}\right)^2}{\beta\left(n^k_p + n^k_{CC}\left(\frac{\alpha_1^2}{x_{CC}}\right) + n^k_{AC}\left(\frac{\alpha_2^2}{x_{AC}}\right) + n^k_{NC}\left(\frac{\alpha_3^2}{x_{NC}}\right) + n^k_{AA}\left(\frac{\gamma^2}{x_{AA}}\right)\right)}, \tag{4}$$

where α_1 represents the fraction of $\pi^+\pi^-$ Coulomb-interacting pairs, the sum $\alpha_2 + \alpha_3$ that of non-Coulomb pairs, and γ the atom pair fraction. It should be noted that α_2 represents specifically the fraction of accidental pairs, which was fixed to the experimentally observed values determined from the spectrum in fig. 2. Minimization was carried out in $(0.5\times0.5)\ (\mathrm{MeV}/c)^2$ bins over the entire (Q_T, Q_L)-plane, under the constraint $\alpha_1+\alpha_2+\alpha_3+\gamma = 1$, with α_3 and γ as free parameters. The β parameter, which represents the overall Monte Carlo normalisation, is actually determined by the number of prompt events in the domain under fit, and it does not need to be varied. The $\alpha_3 = 1 - \alpha_1 - \alpha_2 - \gamma$ fraction then measures the long-lifetime component.

We define the atom signal as the difference between the prompt spectrum and the Monte Carlo with the pionium component (AA) removed. This 2D signal, which reveals the excess with respect to the calculated Coulomb interaction enhancement is compared with the Monte Carlo prediction for atom production. The difference between the two is shown in fig. 3 under the form of a lego plot, where a signed transverse component Q_{xy} has been defined by projecting the measured value of Q_T over a randomly selected azimuth ϕ ($Q_{xy} = Q_T \cos\phi$).

In fig. 4 the p-integrated Q_T spectrum is shown, together with the Monte Carlo and the atom signal extracted from their difference. The longitudinal spectrum is displayed in fig. 5 as well as that of the relative momentum magnitude Q. The observed atom signal is confined to the $Q_L < 2\,\mathrm{MeV}/c$ region as expected from Monte Carlo, whereas the Q_T distribution is wider, due to the larger effect of multiple scattering in the transverse projection.

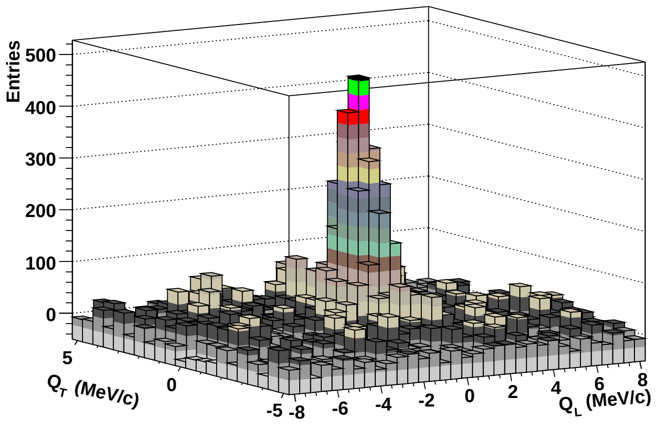

Fig. 3. Lego plot showing pionium break-up in the $(Q_T, Q_L = |Q_Z|)$-plane.

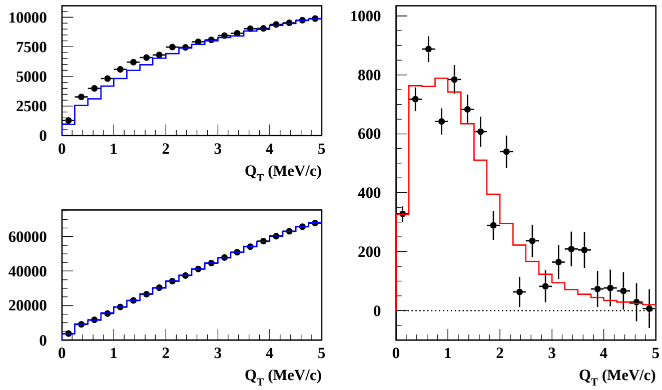

Fig. 4. (Colour on-line) Two-dimensional fit projection onto Q_T. The data are shown separately for $Q_L < 2\,\mathrm{MeV}/c$ (top left) and $Q_L > 2\,\mathrm{MeV}/c$ (bottom left). The difference between prompt data (dots) and Monte Carlo (continuous blue line) is amplified and compared with the pionium Monte Carlo production as red line (right).

5 Breakup probability and pionium lifetime

Once the number of observed atom pairs n_A, and the number of background Coulomb pairs N_C have been determined from the fit in the same kinematical region (by means of the α_1 parameter), pionium breakup probabilities P_{Br} can be determined by using the concept of K-factors. The P_{Br} has been defined as the ratio of n_A over the number of pionium pairs originally produced by the final-state interaction N_A, $P_{Br} = n_A/N_A$. The number of atoms N_A produced in a given phase-space volume is analytically calculated in quantum mechanics and can be related to the number N_C of produced Coulomb pairs by means of the theoretical K-factor:

$$K^{th} = \frac{N_A}{N_C} = 8\pi^2 Q_0^2 \frac{\sum_1^\infty \frac{1}{n^3}}{\int A_C(Q)\mathrm{d}^3Q}, \tag{5}$$

where $Q_0 = \alpha M_\pi$ is two times the atom Bohr momentum p_B. However, the direct measurement obtained in DIRAC for n_A and N_C has been influenced by several reconstruction biases, and that is why we define the experimental

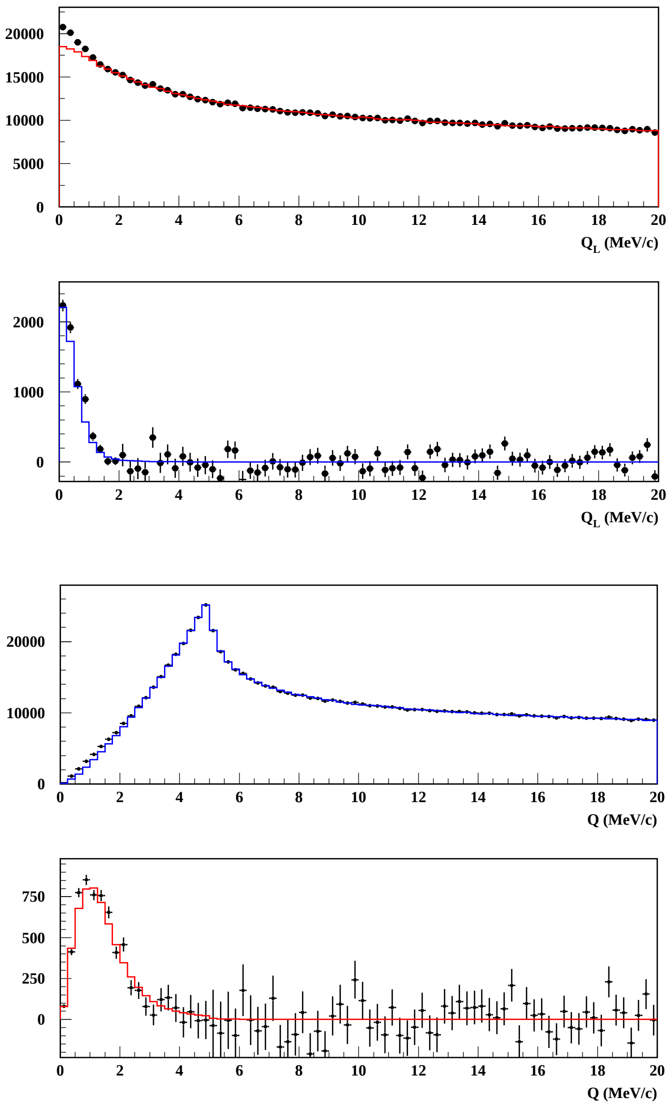

Fig. 5. Two-dimensional fit projection onto Q_L (top panels). The difference between prompt data (dots) and Monte Carlo (line) is amplified at the bottom, where the signal is compared with the pionium atom production Monte Carlo. Projection onto Q is displayed in the bottom panels

K-factor as $K^{exp}(\Omega) = K^{th}(\Omega)\epsilon_A(\Omega)/\epsilon_C(\Omega)$, where ϵ_A and ϵ_C represent the efficiency of the reconstruction chain for atoms and Coulomb pairs, respectively, in a given kinematical region Ω. The P_{Br} is then determined as

$$P_{Br} = \frac{n_A}{N_C K^{exp}(\Omega)}\,. \tag{6}$$

The chosen domain $Q_T < 5\,\mathrm{MeV}/c$ and $Q_L < 2\,\mathrm{MeV}/c$ ensures that the pionium signal is entirely contained.

Figure 6 shows the measured breakup probability as a function of the atom momentum. P_{Br} values are compatible with a smooth increase with increasing atom momentum, as predicted by Monte Carlo tracking inside the target foil [8]. The $1s$ pionium lifetime (τ_{1s}) and statistical error can then be determined by χ^2 minimization with respect to the latter prediction, having τ_{1s} as the only

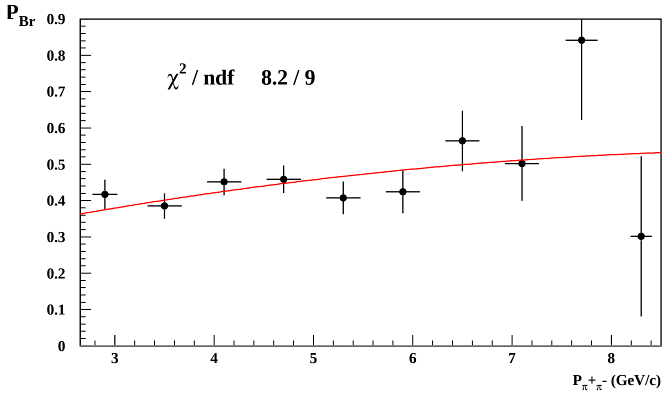

Fig. 6. Pionium break-up probabilities as a function of atom momentum, as compared to best fit Monte Carlo prediction with average Ni foil thickness ($\tau_{1s} = 2.58\,\mathrm{fs}$).

free parameter. Alternatively, the individual P_{Br} measurements at each momentum bin can be combined with independent statistical errors.

6 Systematic error

We have studied the magnitude of possible systematic errors in the measurement of breakup probability, which are summarized in table 1. Generally, they are associated with imperfections of the Monte Carlo simulations of the performance of the apparatus. Given the fact that these are tuned with actual spectrometer data in all cases, the uncertainty ultimately comes from the quality and consistency of a certain number of reference distributions. Concerning the atom propagation inside the target foil, the description of breakup probability is achieved with 1% precision [8]. ω, η' and finite-size nuclear effects on the Coulomb interaction spectrum [9] have been taken into account as a small correction to the CC Monte Carlo spectrum ($\Delta P_{Br} = -0.01$ on average). Its related uncertainty has been estimated by changing the ω fraction by $\pm 25\%$. The material budget of the upstream arm is known to 1.5% precision [10] and furthermore the utilization of the first planes of the MSGC/GEM detector significantly reduces its influence in the measurement. Small biases in Q_L trigger acceptance have been corrected by means of accidental pairs, the corresponding precision being lim-

Table 1. Estimated contributions to systematic error on P_{Br} from the most relevant sources.

Source	σ
Multiple scattering angle	$\pm\,0.003$
Q_L trigger acceptance	$\pm\,0.007$
Simulation of MSGC background	$\pm\,0.006$
Double-track resolution simulation	$\pm\,0.003$
Atom signal shape	$\pm\,0.003$
Finite-size effects and η'/ω contamination	$\pm\,0.003$
Total	0.009

ited by statistics (specially at large momentum). The error estimates in table 1 correspond to maximum reasonable variations, until contradiction with specific reference distributions is encountered. They have been statistically combined, by convoluting step functions defined within the indicated error limits, to provide an overall systematic error in the P_{Br} of ± 0.009, which can be used as a 1σ estimate. This error has been converted into an asymmetric lifetime error $\Delta\tau_{1s} = ^{+0.15}_{-0.14}$ fs using the Monte Carlo propagation code.

A contamination of K^+K^- pairs in the 2001 $\pi^+\pi^-$ data sample has been studied and it appears to be $(2.38 \pm 0.35) \times 10^{-3}$ at $p = 2.9\,\mathrm{GeV}/c$. The Coulomb spectrum of K^+K^- is known and this originates a small correction to τ_{1s}, with negative sign. Another small correction (with positive sign) is also necessary, due to a slight lower-Z contamination in the target foil. Both topics are being finalized at the moment of writing these proceedings, and the overall systematic uncertainty is not expected to increase significantly, as a result of these studies.

7 Summary

Following the analysis of previous sections, the 1s lifetime of pionium atom has been determined to be $\tau_{1s} = 2.58^{+0.26}_{-0.22}(stat)^{+0.15}_{-0.14}(syst)$ fs. A quadrature of both sources of error yields the combined result

$$\tau_{1S} = 2.58^{+0.30}_{-0.26}\,\mathrm{fs},$$

which can be converted into a measurement of the s-wave amplitude difference $|a_1 - a_0| = 0.280\,^{+\,0.016}_{-\,0.014}\ {M_\pi}^{-1} = (0.280 \pm 0.015)\ {M_\pi}^{-1}$.

Minor corrections to the previous measurement are still being investigated before a completely final result will be issued.

We thank the DIRAC Collaboration as a whole for the use of these data. We would like to acknowledge the funding received from the spanish Ministery of Education and Science (MEC), under projects AEN99-0488 and FPA2005-06441, and from the PGIDT of Xunta de Galicia under project PXI20602PR. This publication would not have been possible without the strong computing support received from Centro de Supercomputación de Galicia (CESGA). We thank in particular Carlos Fernández Sánchez, in charge of the SVGD cluster at CESGA, and Andrés Gómez Tato. Our special gratitude to J.J. Saborido Silva and M. Sánchez Garcia, for helping the implementation of our GRID computing strategy. We are also endebted to Cibrán Santamarina Rios for advice concerning his pionium propagation code, as well as to Valery Yazkov for clarification of momentum resolution aspects in DIRAC.

References

1. J. Gasser, V.E. Lyubovitskij, A. Rusetsky, A. Gall, Phys. Rev. D **64**, 016008 (2001).
2. G. Colangelo, J. Gasser, H. Leutwyler, Nucl. Phys. B **603**, 125 (2001).
3. J.R. Peláez, F.J. Ynduráin, Phys. Rev. D **71**, 074016 (2005).
4. J. Nieves, E. Ruiz-Arriola, Eur. Phys. J. A **8**, 377 (2000).
5. B. Adeva *et al.*, DIRAC proposal, CERN/SPSLC 95-1, SPSLC/P 284 (1994).
6. DIRAC Collaboration (B. Adeva *et al.*), Phys. Lett. B **619**, 50 (2005).
7. DIRAC Collaboration (B. Adeva *et al.*), Nucl. Instrum. Methods A **515**, 467 (2003).
8. C. Santamarina *et al.*, J. Phys. B **36**, 4273 (2003).
9. R. Lednicky, nucl-th/0501065.
10. B. Adeva, A. Romero Vidal, O. Vázquez Doce, *Study of Multiple Scattering in Upstream Detectors in DIRAC*, DIRAC Note 05-16, http://dirac.web.cern.ch/DIRAC/i_notes.html.